Title
Energetic ion diagnostics using neutron flux measurements during pellet injection

Journal
Nuclear Instruments and Methods in Physics Research Section A Accelerators Spectrometers Detectors and Associated Equipment, 248(2-3)

ISSN
0168-9002

Author
Heidbrink, WW

Publication Date
1986-08-01

DOI
10.1016/0168-9002(86)91038-7

Nuclear Instruments and Methods in Physics Research A248 (1986) 491–498
North-Holland, Amsterdam

ENERGETIC ION DIAGNOSTICS USING NEUTRON FLUX MEASUREMENTS DURING PELLET INJECTION

W.W. HEIDBRINK

Plasma Physics Laboratory, Princeton University, Princeton, New Jersey, USA

Received 30 December 1985

Neutron measurements during injection of deuterium pellets into deuterium plasmas on the tokamak fusion test reactor (TFTR) indicate that the fractional increase in neutron emission about 0.5 ms after pellet injection is proportional to the fraction of beam–plasma reactions to total fusion reactions in the unperturbed plasma. These observations suggest three diagnostic applications of neutron measurements during pellet injection: (1) measurement of the beam–plasma reaction rate in deuterium plasmas for use in determining the fusion Q in an equivalent deuterium–tritium plasma, (2) measurement of the radial profile of energetic beam ions by varying the pellet size and velocity, and (3) measurement of the "temperature" of ions accelerated during wave heating.

1. Introduction

Injectors that fuel the plasma with solid hydrogenic pellets [1] are in use in most large tokamak experiments. On the tokamak fusion test reactor (TFTR), initial experiments with deuterium pellet injection were conducted early in 1985 [2]. During these experiments, measurements of the d(d, n) neutron emission were made with two stilbene scintillators [3] mounted at different toroidal locations just outside the tokamak vacuum vessel. Studies of the physics of pellet ablation with these scintillators are reported elsewhere [4]. This paper discusses diagnostic applications of fast neutron measurements during pellet injection. Some of the ideas presented here are analogous to the technique for measuring Z_{eff} described by Vasin et al. [5].

The paper begins with a brief summary of the TFTR observations. Next, application of pellet injection to the problem of extrapolating neutron measurements in a deuterium plasma to the fusion production in an equivalent deuterium–tritium (d–t) plasma is discussed. The d–t equivalent fusion Q ($Q \equiv$ (fusion power produced)/(power deposited)), $Q_{\text{dt}}^{\text{equiv}}$, is important because $Q_{\text{dt}}^{\text{equiv}}$ is often used as a figure-of-merit in evaluating fusion devices. Moreover, accurate determination of $Q_{\text{dt}}^{\text{equiv}}$ can indicate the most effective means of introducing tritium into the tokamak in an actual d–t experiment (i.e., pellet injection for thermonuclear reactions, gas puffing for beam–target reactions, or neutral injection for beam–beam reactions). Next, application of pellet injection to measurement of the radial profile of energetic beam ions is considered. Radial profiles of beam neutrals or ions have been measured previously in tokamaks using charge-exchange recombination spectroscopy [6], collimated 3 MeV proton measurements [7], and collimated 2.5 MeV neutron measurements [8]. Relative to these techniques, the use of fast neutron measurements during pellet injection appears considerably simpler with comparable accuracy. Finally, pellet injection as an alternative to neutron spectroscopy is considered. It is shown that during wave heating, the "temperature" of the deuterium tail can be inferred from flux measurements alone.

2. Experimental observations and interpretation

The time evolution of the neutron flux measured with a plastic scintillator mounted adjacent to the TFTR pellet injector (displaced 18° toroidally) is plotted in fig. 1. When a deuterium pellet is injected into

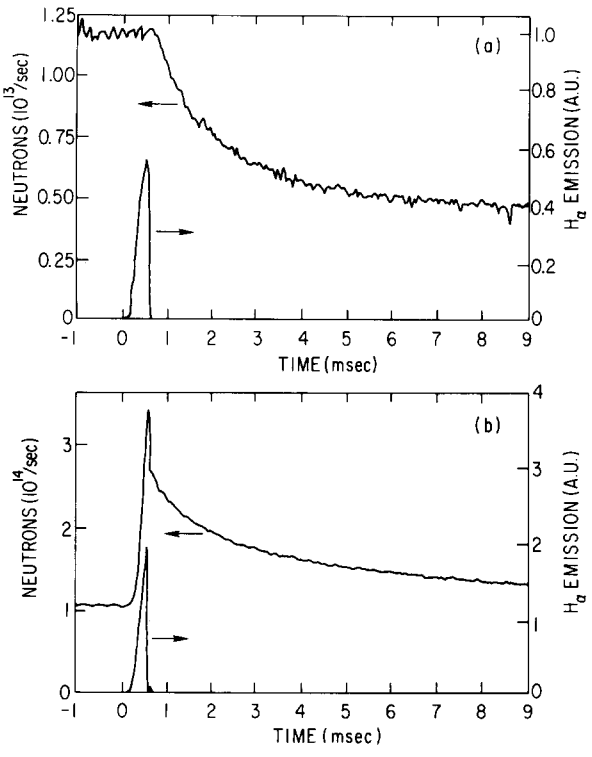

Fig. 1. Neutron emission measured by a plastic scintillator during deuterium pellet injection into an ohmically heated TFTR plasma (a) and into a plasma heated by deuterium neutral beams (b). The H_α signal is used to monitor pellet ablation [9]. The pellet penetrated about 60 cm in the ohmically heated plasma and 44 cm in the beam-heated plasma (the plasma minor radius was $a = 81$ cm).

an ohmically heated deuterium plasma, no spike is observed at the time of pellet ablation and the neutron emission decays with a time constant of about 1 ms to a reduced level (fig. 1a). When a deuterium pellet is injected into a deuterium plasma heated by 80 keV deuterium beams, a large spike in the neutron emission is observed just after the pellet finishes ablating (fig. 1b). A smaller jump in neutron emission is observed by a scintillator situated 126° toroidally from the pellet injector. The signals from the two detectors coalesce (indicating the pellet ions have redistributed toroidally) in 0.1–0.7 ms, depending on the density of the pellet relative to the background plasma density. The neutron emission then decays to a reduced level with a time constant of about 10 ms (only about 1 e-folding time is shown in fig. 1b). Measurements of the redistribution of pellet density perpendicular to the field lines with a five-channel far-infrared interferometer indicate that the characteristic time for radial redistribution of the pellet density is considerably longer (20–100 ms) [10].

In ohmically heated plasmas, the neutron emission is thought to be of thermonuclear origin. No spike in the neutron emission occurs when a pellet is injected into a thermonuclear plasma because the fusion reactivity of the warm Maxwellian distribution with the cold pellet distribution is much less than the reactivity of the warm ion distribution with itself. The reactivity $\overline{\sigma v}(T_1, T_2)$ of two Maxwellian distributions of different temperatures T_1 and T_2 is given by (appendix)

$$\overline{\sigma v}(T_1, T_2) \sim 4.1 \times 10^{-14}(T_1 + T_2)^{-2/3} \exp\left[-24.9(T_1 + T_2)^{-1/3}\right], \tag{1}$$

where T is in keV. For a deuterium temperature $T_d = 2$ keV and pellet temperature $T_p \simeq 0$ keV, $\overline{\sigma v}(T_d, T_d) = 33\overline{\sigma v}(T_d, T_p)$. Since the pellet density about 0.5 ms after ablation is comparable to the initial deuterium density, this implies that the expected jump in neutron yield is of order $1/33 = 3\%$ of the neutron yield prior to pellet injection. The physical explanation for the relatively small reactivity of the

cold pellet ions with the warm deuterons is that most fusion reactions in a thermal plasma occur between ions in the tail of the distribution ($E \simeq 5T_d$) that are traveling in nearly opposite directions. In a sense, fusion reactions in a thermonuclear plasma are "beam–beam" reactions, so it is not surprising that increasing the number of cold deuterons by injecting a pellet does not significantly affect the reaction rate.

In the beam-heated plasma of fig. 1b, the neutron emission increased by about two orders of magnitude when the neutral beams were injected. In this plasma, the fusion production is dominated by beam–target reactions, so adding a pellet to the plasma enhances the reaction rate by rapidly raising the plasma target density.

Collisions between hot ions and the cold pellet plasma reduce the neutron emission on a time scale longer than the time required for the pellet plasma to equilibrate along a field line. Very few ($< 1\%$) 80 keV beam ions strike the solid pellet. Some beam ions ($\sim 10\%$) strike the cold dense pellet plasma before the electrons equilibrate over the flux surface. Since the warm ions that produce thermonuclear reactions are slower than injected beam ions, a smaller fraction ($\sim 4\%$) lose energy in the dense pellet plasma. After the electrons have re-established thermal equilibrium on a flux surface, a warm ion ($E = 5T_d$) slows down due to Coulomb drag in about $\tau_s = 3$ ms, while an 80 keV beam ion slows down in 9 ms. These times are consistent with the experimentally observed decay times of the neutron emission following pellet injection. For the diagnostic applications described below, it is desirable to infer from the actual neutron signal the increase in neutron emission ΔI_n that *would have* occurred in the absence of enhanced Coulomb drag on the fusion-producing ions. The longer time scale for fast-ion equilibration relative to density equilibration implies that ΔI_n can be determined accurately (to within 10%) by using the slope of the neutron emission just after the pellet density has spread over the flux surface to extrapolate the neutron signal back to the time of pellet ablation.

The diagnostic applications described below assume that the time scale for parallel density redistribution $\tau_{\parallel}$ is short compared to the times required for radial density redistribution $\tau_{\perp}$ and for deceleration of the reacting ions τ_s ($\tau_{\parallel} \ll \tau_{\perp}, \tau_s$). These conditions are satisfied in TFTR but have been violated during pellet injection experiments in Alcator C [11].

3. Diagnostic applications

In order to calculate the effect on the neutron emission of injection of a pellet, subdivide the deuterium distribution function into three populations: thermal deuterons (d) of temperature T_d, beam or tail ions (b) produced by neutral beam injection or some other process, and pellet ions (p) of temperature $T_p \simeq 0$. Prior to pellet injection, the pellet density n_p is zero and the neutron yield I_n is

$$I_n = \int \mathrm{d}\boldsymbol{r}\left[\tfrac{1}{2}n_d^2\overline{\sigma v}_{dd} + n_b n_d \overline{\sigma v}_{bd} + \tfrac{1}{2}n_b^2\overline{\sigma v}_{bb}\right], \tag{2}$$

where n_1 is the density of species 1 and the fusion reactivity,

$$\overline{\sigma v}_{12} \equiv \int \mathrm{d}\boldsymbol{v}_1\, \mathrm{d}\boldsymbol{v}_2 f_1(\boldsymbol{v}_1;\, \boldsymbol{r}) f_2(\boldsymbol{v}_2;\, \boldsymbol{r}) \sigma v_{12},$$

is, in general, a function of position $\boldsymbol{r}$. It is convenient to identify separately the three contributions to the fusion emission: the thermonuclear part, I_n^{th}

$$I_n^{th} \equiv \int \mathrm{d}\boldsymbol{r}\tfrac{1}{2}n_d^2\overline{\sigma v}_{dd}, \tag{3}$$

the beam–target part, I_n^{bt},

$$I_n^{bt} \equiv \int \mathrm{d}\boldsymbol{r} n_b n_d \overline{\sigma v}_{bd}, \tag{4}$$

and the beam–beam part, I_n^{bb},

$$I_n^{bb} \equiv \int d\boldsymbol{r} \tfrac{1}{2} n_b^2 \overline{\sigma v}_{bb}. \tag{5}$$

Immediately after pellet injection, the fast part of the thermal deuterium distribution and the beam-ion distribution change little (sect. 2), so

$$I_n^{post} \simeq I_n + \int d\boldsymbol{r} \left[n_p n_d \overline{\sigma v}_{pd} + n_p n_b \overline{\sigma v}_{bp} + \tfrac{1}{2} n_p^2 \overline{\sigma v}_{pp} \right] \simeq I_n + \int d\boldsymbol{r} n_p n_b \overline{\sigma v}_{bp}, \tag{6}$$

since $\overline{\sigma v}_{pd} \ll \overline{\sigma v}_{dd}$ (sect. 2) and $\overline{\sigma v}_{pp} \simeq 0$. Therefore, the change in neutron emission, $\Delta I_n \equiv I_n^{post} - I_n$, is

$$\Delta I_n \simeq \int d\boldsymbol{r} n_p n_b \overline{\sigma v}_{bp}. \tag{7}$$

Define reactivity-weighted beam densities $\tilde{n}_b$ and $\hat{n}_b$:

$$\tilde{n}_b \equiv \frac{\overline{\sigma v}_{bp}}{\langle \overline{\sigma v}_{bp} \rangle} n_b \quad \text{and} \quad \hat{n}_b \equiv \frac{\overline{\sigma v}_{bd}}{\langle \overline{\sigma v}_{bd} \rangle} n_b, \tag{8}$$

where $\langle \overline{\sigma v}_{bp} \rangle$ is the spatially averaged reactivity and $\overline{\sigma v}_{bp}$ is the true reactivity at position $\boldsymbol{r}$. Usually, $\hat{n}_b \simeq \tilde{n}_b \simeq n_b$ since, for classical slowing down, the shape of the velocity distribution function for full-energy beam ions is nearly independent of position. The reactivity of beam ions with thermal deuterons, $\overline{\sigma v}_{bd}$ is, in general, a function of position since the deuterium temperature depends on position but, for $T_d \ll W_b$, where W_b is the beam injection energy, the dependence is weak. Manipulating eqs. (4), (8), and (7) yields the desired result relating the jump in neutron emission $\Delta I_n / I_n$ to the fraction of beam–target reactions I_n^{bt}/I_n, and to the beam-ion, pellet, and thermal densities,

$$\frac{\Delta I_n}{I_n} \simeq \frac{I_n^{bt}}{I_n} \frac{\langle \overline{\sigma v}_{bp} \rangle}{\langle \overline{\sigma v}_{bd} \rangle} \frac{\int d\boldsymbol{r} n_p \tilde{n}_b}{\int d\boldsymbol{r} n_d \hat{n}_b}. \tag{9}$$

The use of eq. (9) in various limits is discussed in the following subsections.

3.1. Q_{dt}^{equiv} determination

The reaction rate I_{dt}^{equiv} in an "equivalent" d–t experiment is related to the measured reaction rate I_n in the actual d–t experiment by

$$I_{dt}^{equiv} = a_{th} I_n^{th} + a_{bt} I_n^{bt} + a_{bb} I_n^{bb}, \tag{10}$$

where the coefficients a_i depend on the ratio of the t(d, n) to d(d, n) cross section and on the assumed fraction of tritium η[$\eta \equiv$ (hypothetical tritium)/(actual deuterium density)] and deuterium in the hypothetical experiment. For example, the coefficient for the thermonuclear term a_{th} is

$$a_{th} = 2\eta(1-\eta) \frac{\overline{\sigma v}_{dt}}{\overline{\sigma v}_{dd}}. \tag{11}$$

In general, $a_{th} \neq a_{bt} \neq a_{bb}$, since the ratio between the d–t and d–d reactivities depends on the ion distribution function and since the weighting of the tritium and deuterium densities is different for each coefficient. In evaluating I_{dt}^{equiv}, the thermal and beam tritium concentrations are treated as free parameters and optimized to achieve the maximum value of I_{dt}^{equiv}. After optimization with respect to the density, the three coefficients a_{th}, a_{bt}, and a_{bb} can be accurately evaluated to within 10% but typically differ from one

another by 50%. This implies that, for accurate evaluation of the equivalent Q_{dt}^{equiv} ($Q_{dt}^{equiv} \propto I_{dt}^{equiv}$), separate measurements of I_n^{th}, I_n^{bt}, and I_n^{bb} are needed.

At moderate to high plasma densities the beam–beam reaction rate I_n^{bb} is usually small compared to the beam–target reaction rate I_n^{bt}; with beam injection at low densities, the thermonuclear rate I_n^{th} is often negligible. This implies that simultaneous measurement of the total reaction rate I_n by conventional means and of the beam–target fraction I_n^{bt}/I_n through pellet injection (eq. (9)) permit accurate evaluation of I_{dt}^{equiv} in eq. (10). The accuracy of measurement of I_n^{bt}/I_n through eq. (9) depends mainly on the accuracy of determination of the various densities n_p, n_b, and n_d. The jump in neutron emission $\Delta I_n/I_n$ typically can be measured to 10%. For deuterium neutral beam injection, the beam energy W_b is usually much larger than the thermal deuterium temperature T_d ($W_b \ll T_d$) and the ratio of reactivities appearing in eq. (9) is

$$\frac{\langle \overline{\sigma v}_{bp} \rangle}{\langle \overline{\sigma v}_{bd} \rangle} = 1 + O(T_d/W_b),$$

which implies that this term is known to $\sim \pm 5\%$. The deuterium density n_d is not directly measured in tokamaks. For moderately low Z_{eff} and moderate density so that $n_d \gg n_b$, the deuterium density profile can be deduced fairly accurately from the electron density measured by Thomson scattering (or other means). At very low densities such that $n_d = O(n_b)$, the deuterium density cannot be determined accurately from the electron density; however, pellet measurements in this regime are still valuable to verify that the plasma is truly in the regime where beam–beam reactions dominate. The pellet density profile n_p can be deduced directly from electron density measurements made shortly (~ 1 ms) after pellet injection, using the fact that $n_p = \Delta n_e$ for a $Z = 1$ pellet. Alternatively, measurements of the H_α emission (using the usual assumption that the ablation rate is proportional to the emitted light), together with the assumption that all the mass is deposited in the plasma, could be used to infer n_p. The least accurately known quantity in eq. (9) is usually the density of full-energy beam ions, n_b, which is generally calculated using beam-deposition codes. Note, however, that although n_b is itself highly uncertain, the sensitivity of the deduced beam–target rate I_n^{bt}/I_n is much less uncertain since errors in n_b tend to be averaged out by the integration $\int dr n_b n_{d,p}$. Note, too, that the integral over n_b appears in both the numerator and the denominator of eq. (9). In fact, if the pellet deposition profile $n_p(r)$ can be chosen to approximate the deuterium density profile $n_d(r)$, the dependence on n_b largely cancels out. Alternatively, one can attempt to determine the sensitivity to beam profile by varying the pellet deposition (sect. 3.2). In conclusion, at moderate to high densities with central pellet deposition, it should be possible to measure I_n^{bt}/I_n to about 25% accuracy, which typically implies an accuracy in determining Q_{dt}^{equiv} of about 20% (assuming the absolute accuracy in measuring I_n is 15%). At very low densities, the achievable accuracy in determining I_n^{bt}/I_n is probably only about a factor of 2 but, in this regime, determination of I_{dt}^{equiv} from flux measurements alone is also highly uncertain, so the measurement is still valuable. Furthermore, although Q_{dt}^{equiv} is useful as a figure of merit, the real value of these measurements is to determine the actual mix of fusion reactions in order to guide the physical interpretation of the experiment and to select the most judicious means of adding tritium to the device in an actual d–t experiment.

3.2. Beam-ion profile

At moderate density and moderate ion temperature, the neutron emission during high voltage neutral beam injection is dominated by beam–target reactions ($I_n^{bt}/I_n \simeq 1$). For the sake of discussion, consider the typical case sketched in fig. 2: the deuterium density profile is relatively broad, the beam-ion profile is centrally peaked, and the pellet ablates before traveling to the center of the plasma, reaching a minimum radius $r = r_{ablat}$ (fig. 2). For this case, $\int dr n_p \tilde{n}_b \simeq \Delta N_e \tilde{n}_b(r_{ablat})$, where ΔN_e is the number of pellet electrons deposited in the volume near $r = r_{ablat}$. Thus, eq. (9) can be rewritten

$$\tilde{n}_b(r_{ablat}) \simeq \frac{\Delta I_n}{I_n} \frac{\langle \overline{\sigma v}_{bd} \rangle}{\langle \overline{\sigma v}_{bp} \rangle} \frac{\int dr n_d \hat{n}_b}{\Delta N_e}; \qquad \tilde{n}_b(r_{ablat}) \propto \frac{\Delta I_n/I_n}{\Delta N_e}. \tag{12}$$

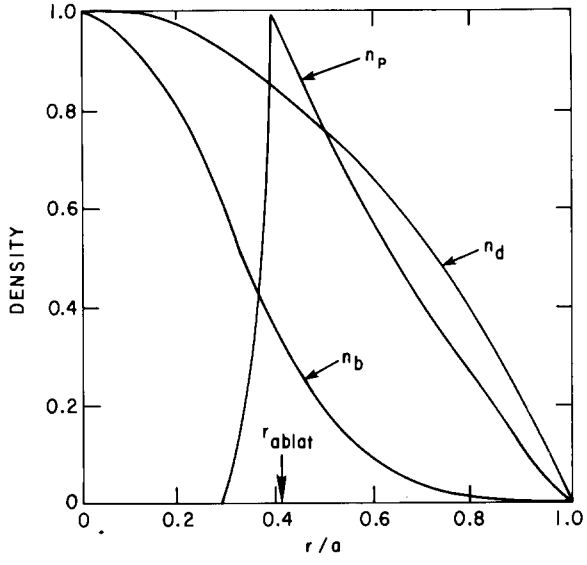

Fig. 2. Sketch of the beam density (n_b), pellet density (n_p), and thermal deuterium density (n_d) profiles. The pellet penetration depth (r_{ablat}) is varied shot-to-shot to measure the beam profile.

The radius of pellet ablation r_{ablat} can be varied by varying the pellet velocity and size [1]. To measure the beam-ion profile, one could establish a reproducible condition and vary the pellet ablation radius shot-to-shot. Measurements of the jump in neutron emission $\Delta I_n/I_n$ and of the electron density ΔN_e would then yield a beam-ion density profile through eq. (12). The shape of the profile could probably be determined to 20%; the absolute accuracy would be much poorer since it depends on absolute measurements of the neutron emission and electron density, and on the calculated beam–pellet reactivity, $(\overline{\sigma v}_{bp})$.

During ICRF heating of a deuterium plasma with a small amount of ^{3}He, the ^{3}He ions are accelerated to large energies and produce d(^{3}He, p) beam–target reactions [12]. To diagnose the energetic ^{3}He profile at the midplane, one could measure the jump in 15 MeV proton emission (which is analogous to $\Delta I_n/I_n$ in eq. (9)) during deuterium pellet injection. The profile obtained by varying the pellet size or velocity could then be used to infer the power deposition profile of the ICRF.

3.3. Tail temperature

During lower hybrid heating (LHH) of deuterium plasmas, an ion tail can form that enhances the neutron yield by up to two orders of magnitude. Under these conditions (and under similar conditions with other forms of wave heating), relatively few particles are accelerated by the wave so that beam–target reactions dominate beam–beam reactions ($I_n^{bb} \ll I_n^{bt}$). The balance of wave acceleration against Coulomb drag tends to produce a tail distribution that is characterized by a "temperature" T_{tail}. There is some experimental evidence for a Boltzmann tail distribution during LHH [13] but, even if the tail distribution is not precisely Maxwellian, T_{tail} can still be used as a convenient measure of typical tail energies. We assume that the pellet penetrates to the magnetic axis and that the tail ion density peaks near the plasma center, which is true during LHH [7,14]. Then $\int d\boldsymbol{r} n_d \tilde{n}_b \simeq n_d(0) N_b$, where N_b is the number of energetic tail ions, and $\int d\boldsymbol{r} n_p \tilde{n}_b \simeq n_p(0) N_b = \Delta n_e(0) N_b$. With the further assumption that the thermonuclear emission originates from the center of the plasma, which is normally the case, we can rewrite eqs. (2), (3), and (9) as

$$\frac{I_n}{I_n^{th}} \simeq 1 + (2n_b/n_d)(\overline{\sigma v}_{bd}/\overline{\sigma v}_{dd}), \tag{13}$$

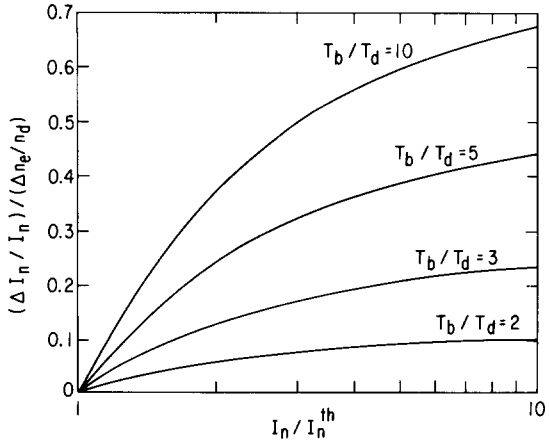

Fig. 3. Normalized jump in neutron emission, $(\Delta I_n/I_n)/(\Delta n_e/n_d)$, vs the ratio of total neutron emission to thermonuclear emission, I_n/I_n^{th}, for various ratios of tail temperature to bulk temperature, T_b/T_d. The curves assume $T_d = 2$ keV but similar curves are found for other temperatures.

and

$$\frac{\Delta I_n/I_n}{\Delta n_e/n_d} \simeq \frac{(2n_b/n_d)(\overline{\sigma v}_{bp}/\overline{\sigma v}_{dd})}{1 + (2n_b/n_d)(\overline{\sigma v}_{bd}/\overline{\sigma v}_{dd})}. \tag{14}$$

Eqs. (13) and (14) constitute two equations for the two unknowns n_b/n_d (the normalized beam density) and T_{tail} (which appears through the reactivities $\overline{\sigma v}_{bp}$ and $\overline{\sigma v}_{bd}$) in terms of the measured quantities I_n/I_n^{th} (the normalized neutron emission), $\Delta I_n n_d/I_n \Delta n_e$ (the normalized jump in neutron emission), and the bulk temperature T_d. Various numerical solutions of these equations are plotted in fig. 3. The various reactivities in eqs. (13) and (14) were evaluated using eq. (1). Fig. 3 indicates that, if the jump in neutron emission upon pellet injection is large, the tail density is low and the effective temperature is high. On the other hand, if the jump is small, the tail distribution is relatively cold and dense.

The results in fig. 3 are not very sensitive to the accuracy of the determination of the bulk temperature T_d. For representative values of $\Delta I_n/I_n$ ($= 0.3$) and I_n/I_n^{th} ($= 3$), doubling the bulk temperature only changes the deduced tail temperature by 20%.

Previously, the tail energy during LHH has been measured using charge exchange and 3 MeV proton spectroscopy [13]. Compared with these techniques, pellet injection appears to be a simple way to detect the presence of a high energy tail and to estimate its energy.

4. Conclusion

In a machine equipped with a pellet injector and an accurate electron density profile diagnostic, scintillator measurements of the jump in neutron emission constitute a simple technique to estimate the temperature of a deuterium tail, measure the profile of fusion-producing beam ions, and accurately determine Q_{dt}^{equiv}.

Acknowledgements

The assistance of T. Deverell, S. Milora, G. Schmidt, K. Young, and the entire TFTR staff in making the neutron measurements of pellet deposition is gratefully acknowledged. A. Ramsey measured the H_α light. J. Strachan made many helpful suggestions. This work was supported by the US Department of Energy Contract No. DE-AC02-76-CHO-3073.

Appendix

Reactivity of a bi-Maxwellian plasma

The derivation of the reactivity $\overline{\sigma v}$ for two Maxwellians follows closely the derivation of the reactivity for distributions of equal temperature [15]. Re-expressing the velocities of particles 1 and 2 in terms of the center of mass (c.m.) and relative velocities and carrying out the integrations over angle and c.m. velocity yields

$$\overline{\sigma v} = \frac{1}{\sqrt{\pi m_1}} \left(\frac{2m_2}{m_1 T_2 + m_2 T_1} \right)^{3/2} \int_0^\infty U \, \mathrm{d}U \sigma(U) \exp\left(\frac{-m_2 U}{m_1 T_2 + m_2 T_1} \right), \tag{15}$$

where $m_{1,2}$ and $T_{1,2}$ are the mass and temperature of particles 1 and 2 and $U = m_1 v^2/2$ is the relative energy. Eq. (15) is exact. At low energies, many cross sections can be approximated by the Gamow form,

$$\sigma(U) \simeq \frac{C_2}{U} \exp\left(-C_1/\sqrt{U} \right). \tag{16}$$

For low temperatures, the argument of the integrand in eq. (15) peaks strongly for some value $U = U_0$ and the integral may be approximated using asymptotic analysis [16]. The result is

$$\overline{\sigma v} \sim \frac{2^{13/6}}{\sqrt{3m_1}} \left(\frac{m_2}{m_1 T_2 + m_2 T_1} \right)^{2/3} C_2 C_1^{1/3} \exp\left[-(2^{1/3} + 0.5^{2/3}) C_1^{2/3} \left(\frac{m_2}{m_1 T_2 + m_2 T_1} \right)^{1/3} \right]. \tag{17}$$

Using Miley's fits to the cross section [17], the expression for the d(d, n)^{3}He reactivity is

$$\overline{\sigma v} \sim 4.1 \times 10^{-14} (T_1 + T_2)^{-2/3} \exp\left[-24.9 (T_1 + T_2)^{-1/3} \right], \tag{18}$$

where $\overline{\sigma v}$ is in cm^3/s and T is in keV. Eq. (18) agrees to within 10% with the numerical evaluation of eq. (15) in the range $T = 0.1$–25 keV.

For $T_1 = T_2$, eqs. (17) and (18) have the same functional form as the well-known equation for the reactivity of a Maxwellian plasma [18], but the coefficients give better agreement with numerical calculations [17] of the reactivity.

References

[1] S.K. Combs, S.L. Milora, C.R. Foust, C.A. Foster and D.D. Schuresko, Rev. Sci. Instr. 56 (1985) 1173.
[2] G. Schmidt et al., Proc. 12th European Conf. on Controlled Fusion and Plasma Physics, Budapest (1985) vol. 2, p. 674.
[3] J.D. Strachan et al., Nucl. Fusion 21 (1981) 67.
[4] W.W. Heidbrink et al., Bull. Am. Phys. Soc. 30 (1985) 1520.
[5] N.L. Vasin et al., Sov. J. Plasma Phys. 10 (1984) 650.
[6] S. Suckewer et al., Appl. Phys. Lett. 45 (1984) 236; S. Suckewer et al., Phys. Rev. A22 (1980) 725.
[7] W.W. Heidbrink et al., Plasma Physics Cont. Fusion 28 (1986) to be published.
[8] J.D. Strachan et al., Phys. Lett 66A (1978) 295.
[9] S.L. Milora, J. Fusion Energy 1 (1981) 15.
[10] H. Park et al., Bull. Am. Phys. Soc. 30 (1985) 1386.
[11] M. Greenwald et al., Phys. Rev. Lett. 53, 352 (1984).
[12] R.E. Chrien and J.D. Strachan, Phys. Fluids 26 (1983) 1953; R.E. Chrien et al., Phys. Rev. Lett. 46 (1981) 535.
[13] R.E. Chrien, R. Kaita and J.D. Strachan, Nucl. Fusion 23 (1983) 1399.
[14] J.J. Schuss et al., Nucl. Fusion 21 (1981) 427.
[15] D.J. Rose and M. Clark, Jr., Plasmas and Controlled Fusion (MIT Press, New York, 1961) p. 82.
[16] C.M. Bender and S.A. Orszag, Advanced Mathematical Methods for Scientists and Engineers (McGraw–Hill, New York, 1978) p. 267.
[17] G.H. Miley, H. Towner and N. Ivich, Rept. COO-2218-17 (University of Illinois, Urbana, IL, 1974).
[18] R.F. Post, Rev. Mod. Phys. 28 (1956) 339.